

General performance analysis of a Fizeau interferometer

Sebastian E. Egner^a, Thomas M. Herbst^a, Carmelo Arcidiacono^b

^aMax-Planck-Institute for Astronomy, Königstuhl 17, 69117 Heidelberg, Germany;

^bINAF - Osservatorio Astrofisico di Padova, Vicolo dell'Osservatorio 5, 35122 Padova, Italy;

ABSTRACT

A Fizeau interferometer combines the light of several telescopes to obtain panoramic images with an angular resolution equivalent to the longest edge-to-edge separation in the system. The overall performance of a Fizeau interferometer depends critically on the performance of the (MC)AO system and the efficiency of atmospheric piston correction, but also on other effects like alignment accuracies, filter bandwidths, tracking errors, atmospheric dispersion and field rotation. Due to the mutual dependence, Strehl ratio or fringe contrast like in conventional Adaptive Optics systems or pupil plane interferometers are not sufficient for a concise assessment of the performance of such an instrument. As a measure for the actual performance, we propose to use the ratio R23, which is the actual high-spatial frequency information in the images, divided by what could be measured in principal with a 23m telescope (as the LBT). We present the theoretical concept of this method and show the results of various simulations of the abovementioned effects as an application to LINC-NIRVANA, a Fizeau interferometer currently being built for the LBT.

Keywords: Interferometry, Fizeau Imaging, wavefront error, Adaptive Optics

1. INTRODUCTION

LINC-NIRVANA¹ is a Fizeau interferometer for the LBT and will combine the light from the two 8.4m primary mirrors into one focus. These two primary mirrors are mounted on a common alt-az mount with a center-to-center separation of 14.4m (figure 1). In order to compensate for the atmospheric distortions of the incoming wavefront and to maintain zero OPD between its two arms, LINC-NIRVANA will use a sophisticated MCAO system² and a fringe-tracker.³ Since the coherent combination of the light happens in the focal plane, LINC-NIRVANA will have a very large, compared to Michelson interferometers, field-of-view of $10'' \times 10''$. The resulting PSF (figure 1) is a combination of a 8m PSF, with intersecting fringes corresponding to the 14.4m separation of the two primary mirrors. The diameter of the larger Airy disk is given by $\alpha_{\text{Airy}} = 1.22\lambda/D_{\text{tel}}$, with the single telescope diameter D_{tel} . In contrast the separation of the fringes depends essentially on the separation D_{base} of the two primary mirrors is given by $\alpha_{\text{fringes}} = 1.22\lambda/D_{\text{base}}$. The angular resolution in the image thus corresponds to a 22.8m telescope in the projected direction connecting the two primary mirrors and of an 8m telescope in the perpendicular direction. By combining several images, each taken at a different parallactic angle and thus orientation of the fringes on the sky, the full angular resolution in all directions can then be reconstructed via sophisticated deconvolution algorithms.^{4,5} LINC-NIRVANA will be capable of obtaining diffraction-limited images in the wavelength range from J to K band.^{6,7} With a pixel scale of 0.005''/pixel for Nyquist sampling of the fringes in J-band, the field-of-view is essentially limited by the size of the detector to $10'' \times 10''$.

To evaluate the performance of such an instrument, an appropriate metric is required, which can be used in all phases of the instrument, starting from the design phase, building, testing and finally also operating the instrument on-sky and improving its performance. When designing and manufacturing the instrument, such a metric is required to establish an error-budget in order to derive the specifications of the opto-mechanical component. During the testing and commissioning phase, the performance of the instrument has to be evaluated in order to improve it and determine which component has the largest impact on the performance. And finally when operating the instrument on-sky, such a performance metric is required to decide whether the current performance of the instrument meets the observer's needs and it delivers useful data, or measures have to be taken to improve its performance.

Send correspondence to S.E. Egner, E-mail: egner@mpia.de, phone: +49 (0) 6221 528 221

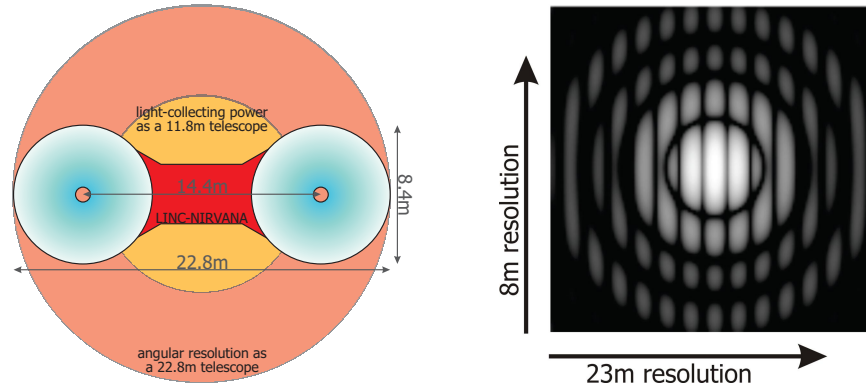


Figure 1. A schematic layout of the LBT with the relevant dimensions and the resulting PSF in log-scale when combining the beams from the two primary mirrors in Fizeau mode (interference in the focal plane).

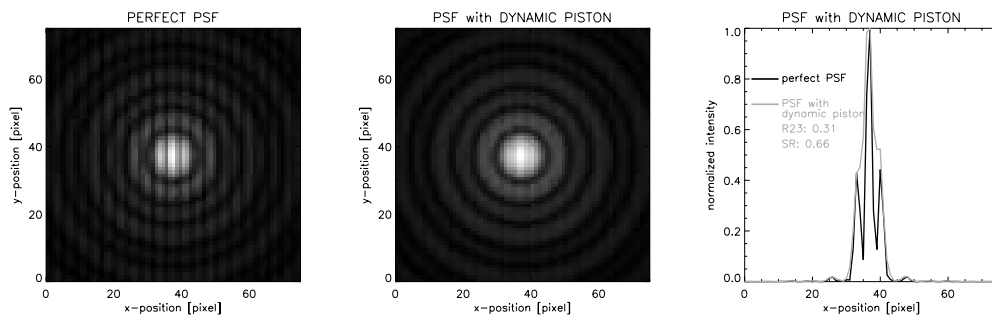


Figure 2. The effect of dynamic piston between the two arms. One can achieve a high Strehl ratio, but only very low fringe contrast. The two pictures on the left are in log-scale.

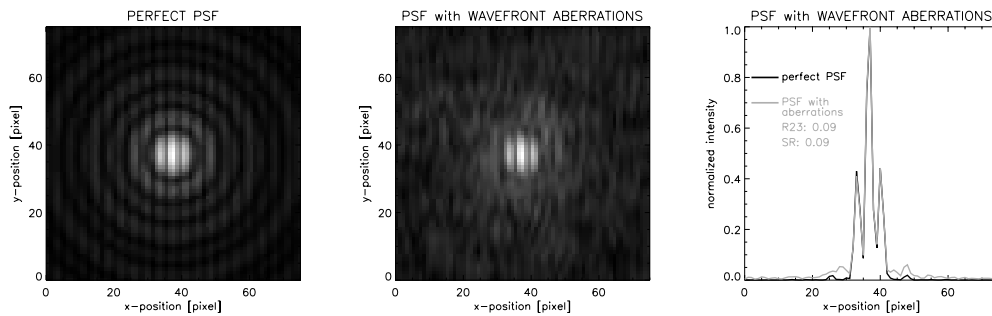


Figure 3. The effect of wavefront aberrations in the two arms. In this case the Strehl is rather low, while the fringe-contrast is still very high. The two pictures on the left are in log-scale.

However, for the performance estimation and evaluation of a Fizeau interferometer, Strehl-ratio like in an imager (which LINC-NIRVANA still is in a certain sense) is not enough. Since LINC-NIRVANA combines the light from the two primary mirrors, not only the wavefronts in the two arms have to be flat, but moreover, in order to achieve the full resolution of a 22.8 m telescope these two wavefronts have to be exact in phase. Figure 2 shows the example of a PSF with a high Strehl ratio, but because of variations of the OPD, no visible fringes. This of course means that the angular resolution is the one of a 8.4 m telescope.

On the other hand, the usual performance measure of Michelson interferometers, the fringe-contrast of a point source, is also not suitable to assess the performance of a Fizeau interferometer. If the two wavefronts

of the two arms are deformed, but deformed in the exactly same way in the two arms, then the interference is strong and thus also the fringe contrast will be high. But of course a deformed wavefront means that the PSF of the image is blurred and thus in turn the angular resolution is low. In figure 3 an example PSF with large wavefront aberrations but still rather high fringe contrast is shown.

What is more, a large number of effects influence the performance of the system, either via the reduction of the single-eye Strehl ratio, or by introducing static or dynamic OPD between the two arms. This includes for example wavefront aberrations (atmospheric, telescope, instrument, etc.), field rotation, piston variations (atmospheric, instrument, tracking errors, etc.), atmospheric dispersion, offsets between the rotation and the optical axis, filter bandwidth, shape of pupil images, flexure inside the instrument, and so on. Traub et al.⁸ presented already a theoretical description of the alignment accuracy of the instrument and the telescope, but it is difficult to extend this method and include also the effects just described in an analytical fashion. Therefore a new and combined performance measure for a Fizeau interferometer is required to assess the impact of all these effects. In this paper we present such a technique and show some applications to LINC-NIRVANA.

2. THEORETICAL CONCEPT

As explained above, the fringe contrast of a point source used in a Michelson interferometer to evaluate the performance of the system is a rather abstract measure and not sufficient for a Fizeau interferometer. A more demonstrative and significant measure for a Fizeau interferometer can be obtained by looking at the transmitted angular frequencies of the instrument. Especially for a Fizeau interferometer the observer is interested in the high angular frequencies, which are not observable with a single telescope. Information in these high angular frequencies can be observed only with the interferometer.

Two good measures to describe the image quality of an optical system are the MTF (modular transfer function) and the PSF (point spread function). The MTF describes how effectively spatial frequencies in the object space are transferred to the image space through the optical system, while the PSF is the resulting image of a point-source. The PSF is defined as the absolute value of the Fourier-transform of the aperture function $\Theta(\mathbf{r})$ (with $\Theta(\mathbf{r}) = 1$ for inside the pupil, and 0 otherwise), with possible wavefront aberrations $A(\mathbf{r})$ being included as a complex weighting function:

$$\mathbf{PSF}(\mathbf{r}) = \left| \mathbf{FT} \left\{ \Theta(\mathbf{r}) \cdot \exp[2\pi i A(\mathbf{r})] \right\} \right|^2 . \quad (1)$$

The MTF is related to the PSF via

$$\mathbf{MTF}(\kappa) = \left| \mathbf{FT} \{ \mathbf{PSF}(\mathbf{r}) \} \right|^2 . \quad (2)$$

This last relation also shows that the MTF is directly related to the image quality quantified by the PSF. If the diameter of the PSF is smaller, then the image is sharper, which can be also represented by an higher quantity of high spatial frequency information in the image and vice versa. The MTF for a 23m telescope is shown in figure 4.

If the shape of the pupil is more complex (like in the case of LINC-NIRVANA, where it is not circular, but consists of two separated primary mirrors), also the MTF gets more complicated. The resulting MTF for LINC-NIRVANA is also shown in figure 4. As explained in the introduction, the LBT is an alt-az mounted telescope and thus the fringes will rotate with respect to the sky. This allows to reconstruct the full angular resolution in all direction, when combining images taken at different parallactic angles. Figure 4 shows the resulting MTF of LINC-NIRVANA, when combining images over 90 degree of parallactic angle change, containing contributions with high angular frequencies at a corresponding interval of directions on sky.

The value of the MTF is reduced by various effects, like wavefront aberrations, piston variations, misalignments and so on, resulting in a blurred image and thus in a reduced angular resolution of the instrument. Since the uniqueness of LINC-NIRVANA is its capability to observe angular frequencies, which are not accessible by the current 8 m class telescopes, the goal is to have as much power as possible in these high angular frequencies. Therefore the best criteria for the performance of LINC-NIRVANA is the size of the two smaller bumps in the MTF shown in figure 5. To quantify this, we define R23 as the ratio between the volume under these smaller

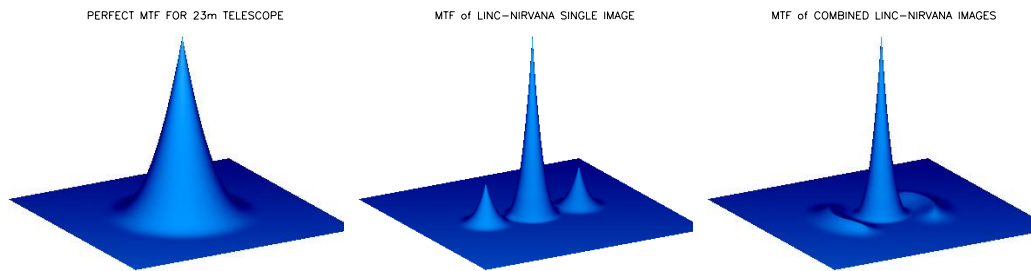


Figure 4. The MTF (modulation transfer function) of a full aperture 23 m telescope (**left**), for a single image of LINC-NIRVANA at the LBT (**middle**) and integrated over a field rotation of 90 degrees (**right**).

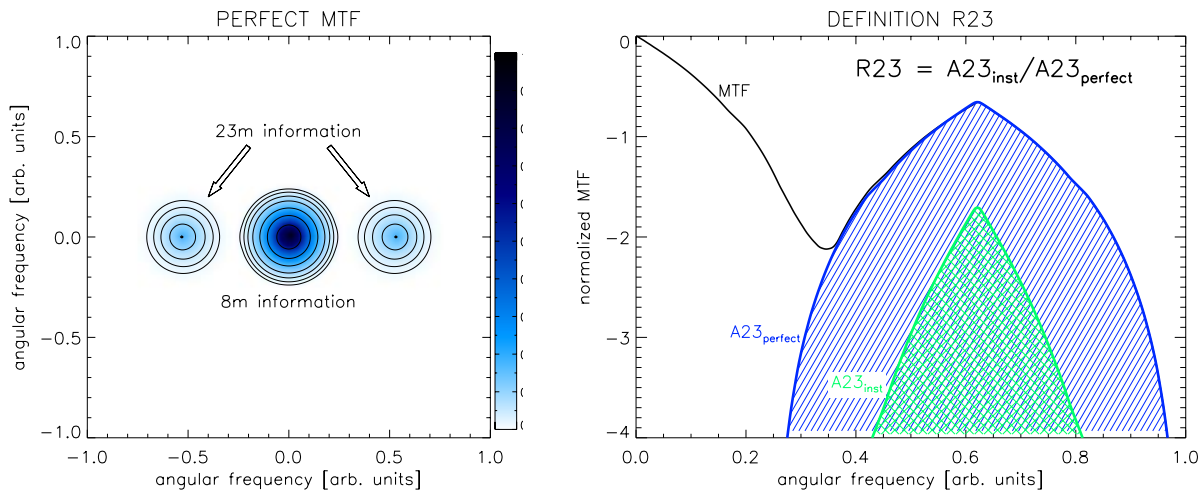


Figure 5. Left: A contour plot of the perfect MTF of LINC-NIRVANA. **Right:** A sketch to illustrate the definition of R23 in the case of LINC-NIRVANA, as the ratio between the area below the actual MTF and the perfect MTF in the outer wings containing the information of a 22.8 m telescope.

bumps of the actual observed image $\mathbf{MTF}_{\text{inst}}$ and that of a perfect telescope and instrument with no atmospheric disturbances $\mathbf{MTF}_{\text{perfect}}$:

$$\text{R23} = \frac{\int_{23\text{m}} \mathbf{MTF}_{\text{inst}} dk}{\int_{23\text{m}} \mathbf{MTF}_{\text{perfect}} dk} . \quad (3)$$

Figure 5 illustrates this concept.

3. SOME APPLICATIONS

Once the concept for the performance analysis has been established, simulations can be performed to quantify the impact of the various effects mentioned in the introduction. According to equation 2, the MTF and thus R23 can be calculated from the Fourier-transformation of the pupil function, with the wavefront aberrations as a complex weighting function. By modifying the pupil geometry or adding some wavefront aberrations, the impact of these effects can thus simulated and analyzed. In this section we will present the results of a few examples of such simulations.

3.1. Wavefront aberrations

As shown in the introductory example shown in figure 3, wavefront aberrations in the optical system result in a blurring of the image and thus reduce the high angular frequency information contained in the obtained

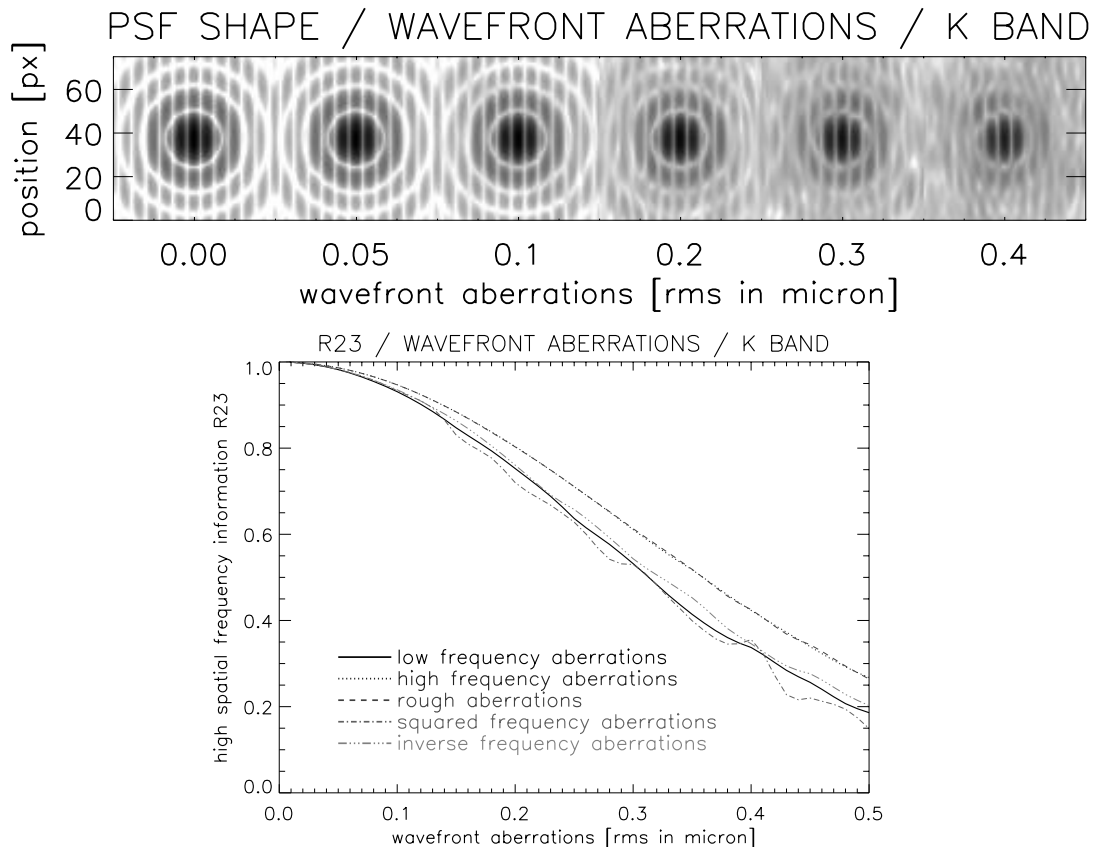


Figure 6. Top: The shape of the PSF in log-scale of LINC-NIRVANA in K band in the presence of wavefront aberrations. **Bottom:** The resulting impact on R23 for various kinds of wavefront aberrations in K band.

images. Random wavefront aberrations with a given power spectral density were included in the complex pupil function (equations 1 and 2) to simulate the resulting PSF and MTF. This procedure was repeated over many realizations with different wavefront aberrations, but with the same power spectral density. All the obtained MTF functions were then averaged and the mean value of R23 determined, like in a real long exposure image. Figure 6 shows the resulting PSFs and MTFs as a function of the RMS of the wavefront aberrations. In these simulations everything else was assumed to be perfect, in particular no OPD variations, no chromatic effects and no misalignments were considered.

As also shown in figure 6, the reduction in R23 does not depend on the spectral distribution of the wavefront aberrations. This means that for example the effect of partial correction of the wavefront distortions by the AO system can be analyzed directly with the results presented here. It is not necessary to include details of the AO system, like for example the correction efficiency of individual modes. Instead, R23 depends only on the residual RMS value of the wavefront aberrations.

3.2. OPD variations

Another major factor limiting the performance of a ground-based interferometer are variations of the piston caused by the atmosphere or telescope. These variations can be considered as wavefront aberrations over scales of several tens of meters and introduce a variation of the OPD between the two arms. As already shown in the introduction (figure 2), such variations can completely destroy the fringe contrast. Even with an AO system working perfectly, the information contained in such images is not more than what could be obtained with a single telescope of the interferometer.

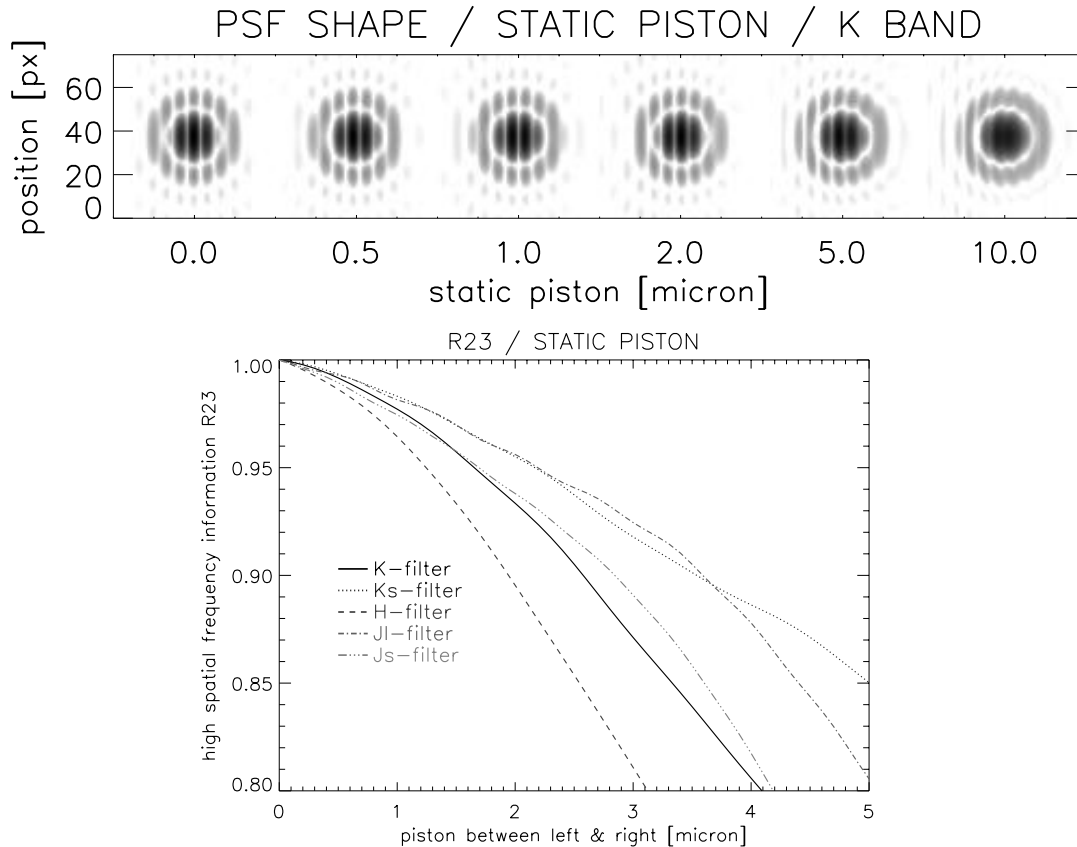


Figure 7. Top: The shape of the PSF in K-band for LINC-NIRVANA for static piston with various amplitudes and a filter bandwidth of 0.4 micron (log-scale). **Bottom:** The reduction in R23 for a static piston in K band as a function of the static piston between the arms.

The reason is that a variation of the OPD between the two arms results in a shift of the fringes with respect to the 8.4 m PSF. If for example the OPD is changing by one wavelength, the position of dark and bright stripes will be (to first order) swapped. If the OPD between the two arms is constantly changing with an amplitude of the order of one wavelength, the fringes will be completely smeared out and the high angular frequency information will be lost. On the other hand, if there is an OPD between the two arms, but it remains constant to within a small fraction of the wavelength, then the impact on the performance of the instrument should be small, as long as the light from the two arms is still coherent. Therefore two cases have to be considered when simulating the impact of variation of the OPD between the two arms. The first case is a variation of the OPD over time-scales, which are much shorter than the integration time. Even small variations of the OPD will then result in a smearing of the fringes in a long exposure. The other case is a static OPD between the two arms. In this case the fringes are shifted, but their position will remain fixed with respect to the 8.4 m PSF. The performance of the instrument is then independent of the exposure time.

The impact of a variation of the OPD between the two arms can be simulated by adding a wavefront aberration consisting of a pure piston to one of the two pupils. The impact of dynamic piston on the average MTF and R23 can be determined by repeating the simulations over many realizations, each with a random piston value following a Gaussian distribution with a given RMS value. The R23 for a dynamic OPD can be determined from the mean MTF of all these realizations, while the impact of a static OPD can be determined by simply analyzing the MTF for each realization individually.

The results of these simulations are shown in figure 7 for a static piston and in figure 8 for dynamical piston

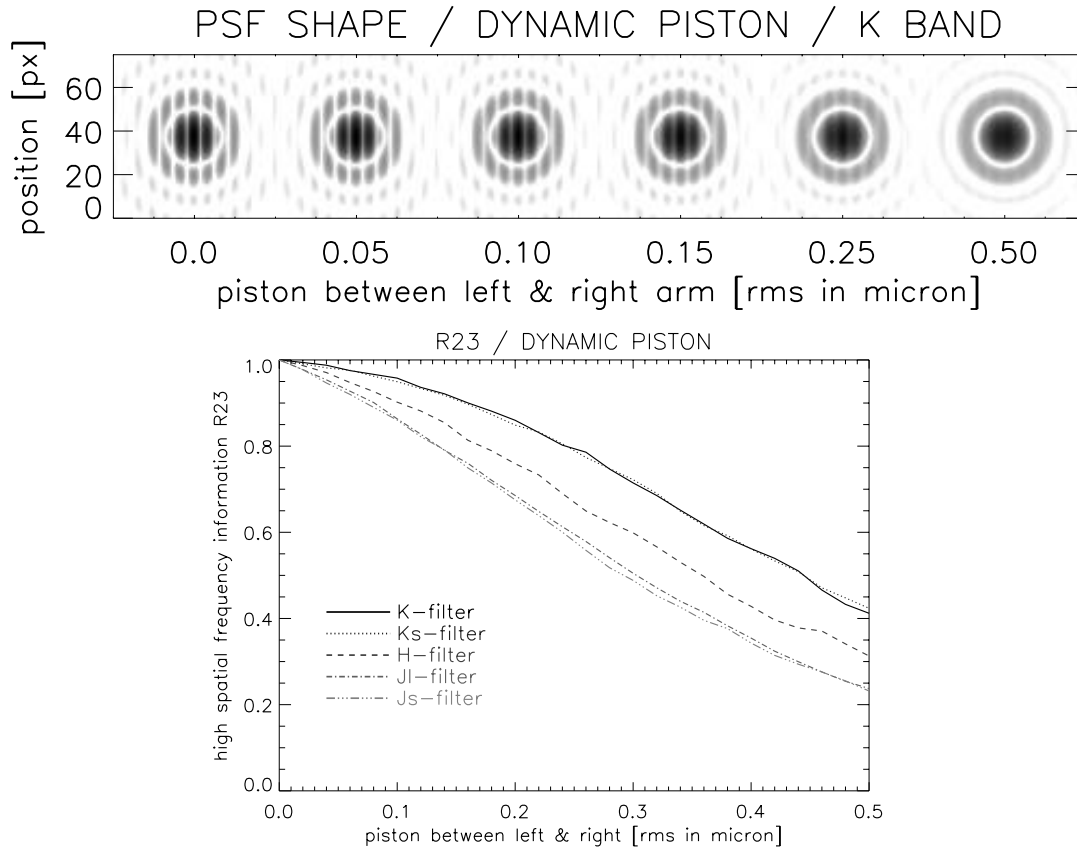


Figure 8. Top: The shape of the PSF in K-band for dynamic piston and various amounts of dynamic piston. **Bottom:** The reduction in R23 for a dynamic piston with the RMS value as indicated.

variations. In the case of static piston, the reduction in R23 depends essentially on the bandwidth of the used filter, while for dynamic piston clearly the center wavelength of the filter is the crucial quantity.

3.3. PSF overlap

LINC-NIRVANA is a Fizeau-interferometer, which means that the actual interference of the beams only happens in the focal plane of the instrument. Therefore it is essential that the two PSFs from the two primary mirrors overlap precisely. Any misalignments will directly reduce the fringe contrast. A non-overlap corresponds to a tilt in one of the two pupils and thus to a very large-scale wavefront aberration causing the PSF to broaden. It can thus simulated by simply adding a tilt to one of the two pupils.

Figure 9 shows the results of the simulations, namely the PSF and the R23 as a function of the shift of one of the two PSFs, both perpendicular and parallel to the fringes. As can be seen in this figure, the impact on R23 is independent on the direction of the shift of the PSF, it only depends on the separation of the two PSFs.

3.4. Tracking errors / Flexure

Another source of performance loss are tracking errors or flexure within the system. Both cause a shift of the PSF on the science detector during the exposure. The result is a smearing of the fringes, especially when the PSF is shifted perpendicular to the fringes. Again, high angular frequency information will be lost.

To simulate these effects, multiple perfect PSFs of LINC-NIRVANA as shown in figure 1 were slightly shifted with respect to each other and then simply added. The average MTF and thus R23 can be calculated from this

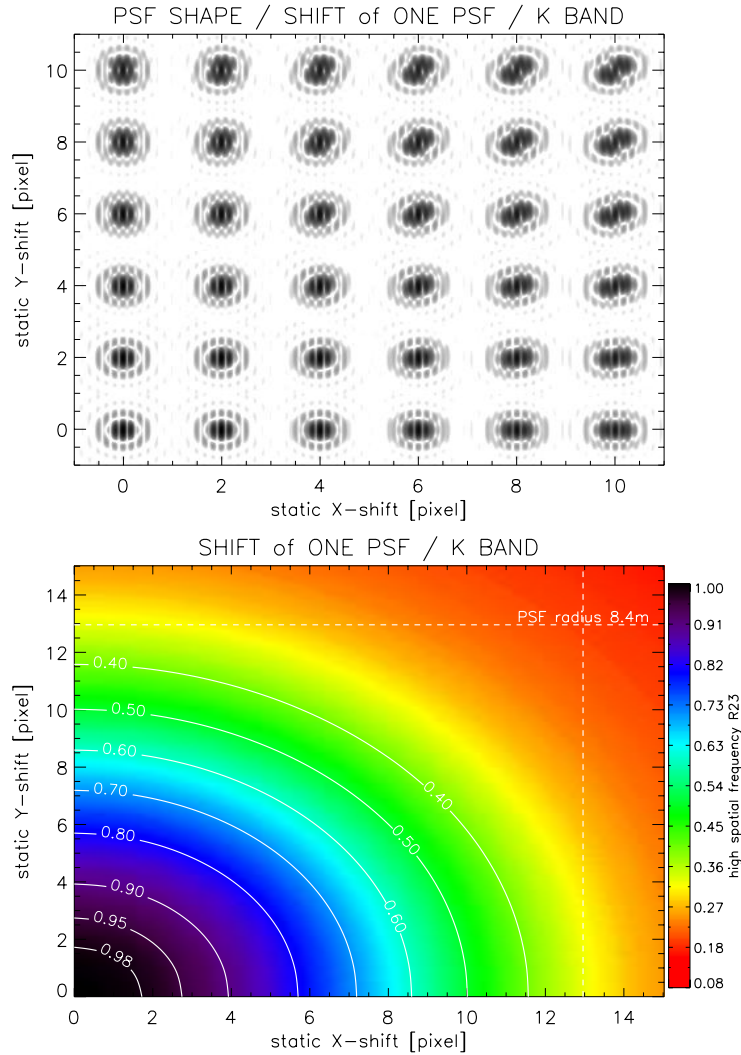


Figure 9. Top: The shape of the PSF for a misalignment of one of the two PSFs in K band (log-scale). **Bottom:** The impact on the R23 as a function of the shift parallel (x-direction) and perpendicular (y-direction) to the fringes.

average PSF by using equations 2 and 3. As figure 10 shows, the reduction in R23 depends critically on the direction of the shift of the PSF. A small shift of a few pixel perpendicular to the fringes completely destroys the fringe contrast and thus the high angular frequency information, while the impact of a shift parallel to the fringes is much less severe.

Tracking errors $\Delta\alpha_{az}$ in the azimuthal direction cause additionally a change of the OPD between the two arms with an amplitude of

$$\text{OPD} = D_{\text{base}} \cdot \sin \Delta\alpha_{az} . \quad (4)$$

Depending on the correction efficiency of the FFTS, a residual OPD error might remain, which causes a reduction in R23 as described in section 3.2.

3.5. Field rotation

There are generally two kinds of rotation in an instrument for an alt-az mounted telescope. One is the rotation of the sky on the detector, the other is the rotation of the pupil (or its image) on the detector. A rotation of

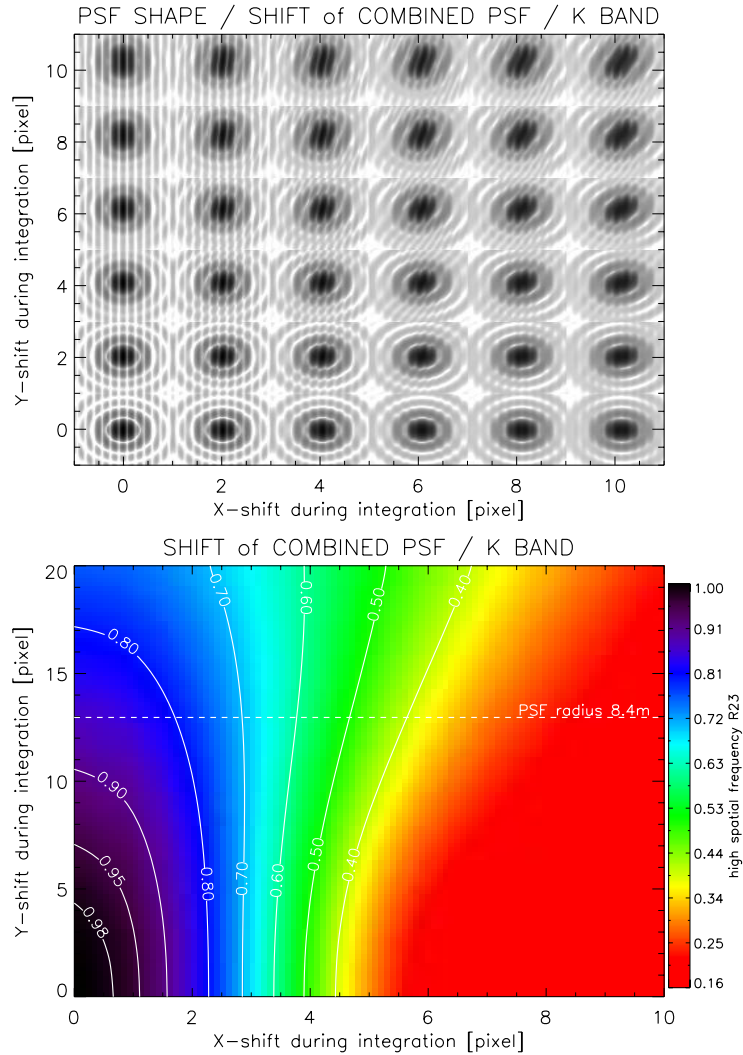


Figure 10. Top: The shape of the PSF in K band for LINC-NIRVANA for a shift of the combined PSF during the integration, caused by flexure or tracking errors (log-scale). **Bottom:** The impact on R23 as a function of the shift parallel (x-direction) and perpendicular (y-direction) to the fringes. Note the different scales for the shift in x- and y-direction.

the sky will move the stars on the science detector, while a rotation of the pupil in LINC-NIRVANA rotates the fringes on the science detector. Since the LBT is an alt-az mounted telescope and the fringes will always be perpendicular to the line connecting the two primary mirrors, they will always be perpendicular to the horizon. However, the sky will rotate on the science detector. To avoid getting images of star trails, the science detector will thus be rotated for compensation. This in turn means that the fringes will rotate on the science detector and thus reduce the fringe contrast in a long exposure image.

To simulate this effect, multiple perfect PSFs of LINC-NIRVANA were simply rotated individually and then added. Similarly to the previous section, the average MTF and R23 can then be calculated from the averaged PSFs. The result as shown in figure 11 indicates that a rotation of less than 10 degree during the exposure has only very little impact on R23. Also shown in figure 11 is the effect of an additional shift between the optical axis (i.e. the rotation axis of the sky) and the rotation axis of the science detector. For an offset between those two axes of 10 pixel (corresponding to 0.05" on-sky or 240 μm in the focal plane) a rotation of 10 degree already reduces R23 by more than 10%.

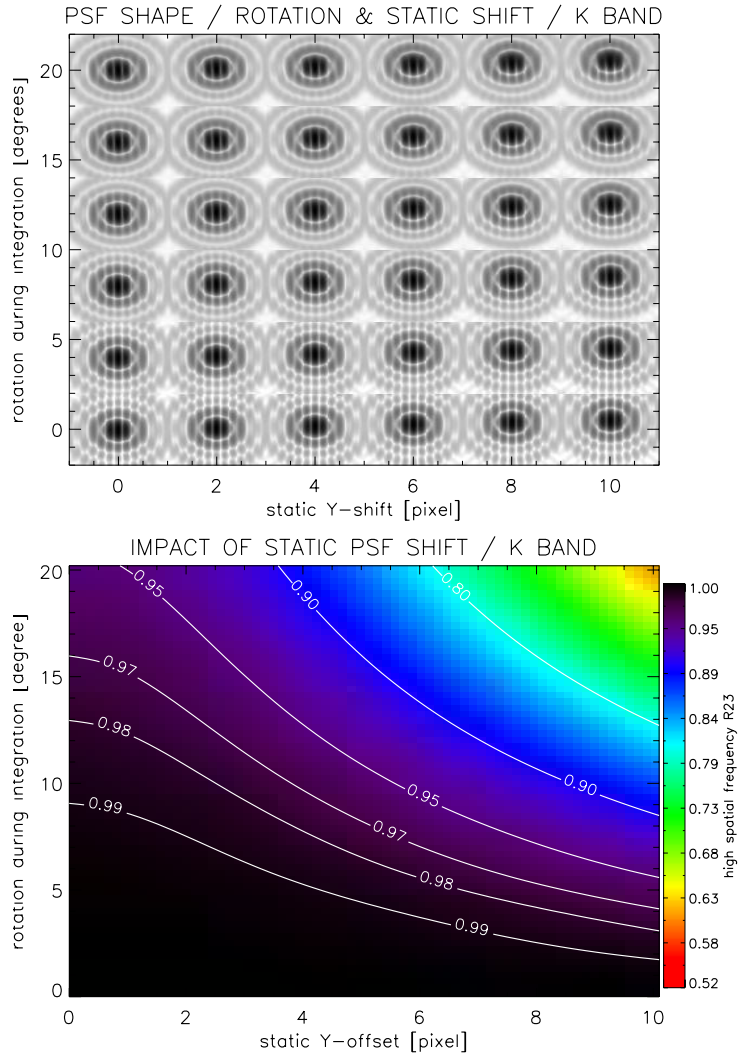


Figure 11. Top: The shape of the PSF in K band for LINC-NIRVANA for a rotation of the field and thus of the detector with respect to the fringes and an offset between the optical axis and the rotation axis of the detector (log-scale). **Bottom:** The impact on R23 as a function the rotation angle during the exposure and the offset between the optical axis and the rotation axis of the detector.

3.6. Filter bandwidth

Another important aspect, which was already mentioned in section 3.2 is the coherence length l_c of the light. It is related to the filter bandwidth $\Delta\lambda$ via

$$l_c = \frac{\lambda^2}{2\Delta\lambda}. \quad (5)$$

A larger coherence length (or smaller filter bandwidth) means therefore that the light still can interfere in the focal plane, even if there is a static OPD in the system.

To illustrate this effect, one has to consider that the separation of the fringes apparent in the PSF of LINC-NIRVANA depends on the wavelength, for shorter wavelength the fringes are closer together. This means that only for the 0th fringe the fringe-packages for the individual wavelengths overlap perfectly. Introducing OPD between the two arms will shift the fringe packages to one side. If for the center wavelength the nth fringe is in the middle of the 8.4 m PSF, then the nth fringe for shorter wavelength will be for example slightly to the left,

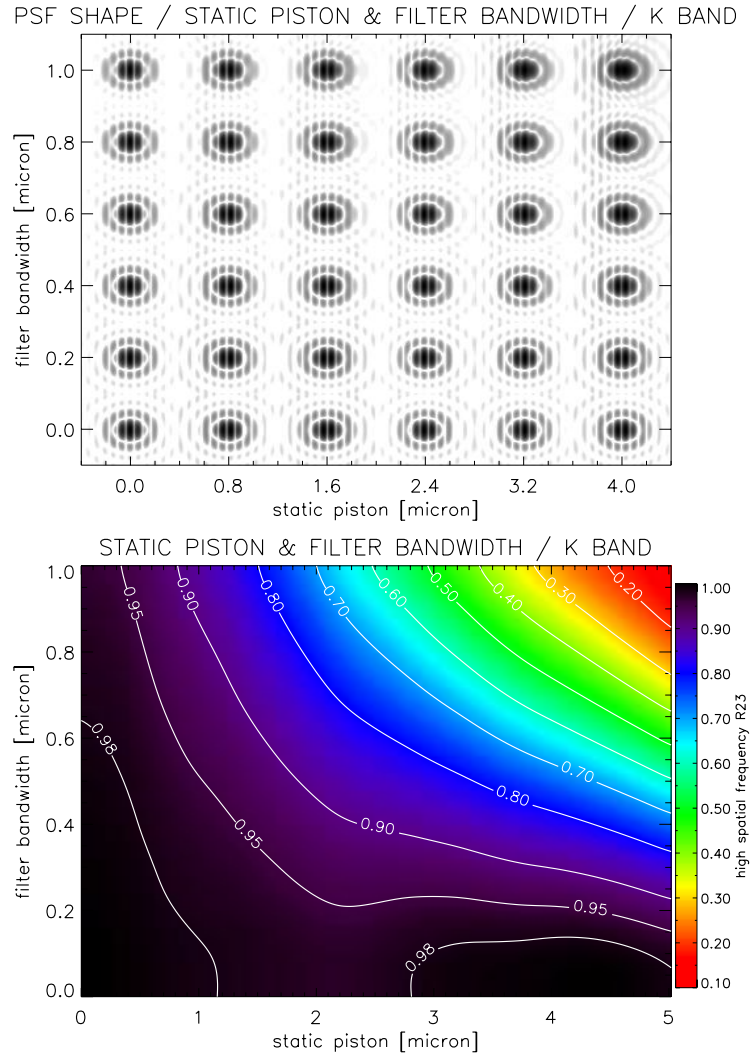


Figure 12. Top: The shape of the PSF as a function of the filter bandwidth, centered on $2.2 \mu\text{m}$, and the amplitude of static piston (log-scale). **Bottom:** The impact on R23 as a function of the static piston between the two arms and the bandwidth of the filter.

while it will be to the right for longer wavelength. Superposing these PSFs for the various wavelengths will then result in a reduction of the fringe contrast, because the dark stripes in the PSF associated to one wavelength will be illuminated by the bright fringes of the PSF associated to another wavelength.

Various PSFs for different wavelengths within the filter were calculated and then added. The average MTF and R23 was then again determined from the obtained average PSF. Figure 12 shows the results, both the PSF and the R23 as a function of static piston and filter bandwidth.

3.7. Shape of pupil images

In this section we will show how the results obtained above can be used to determine also the impact of other effects, in this example the position and shape of the pupil images inside the instrument. In a Fizeau interferometer, there are usually images of the entrance pupils inside the instrument which are then imaged with one common optical system onto the science detector where the beams finally interfere to create the fringes. These

pupil images have to be an exact copy of the entrance pupils, otherwise the PSFs will not overlap off-axis, or there will be a field-dependent OPD.

In the case that the diameter of the two cold pupils are different in the two arms, the plate-scale will be different. The result is that the two images of a star on-axis can well overlap, but that the images of off-axis sources will be separated. The impact of different plate scales can then be derived with the results shown in figure 9. A difference in the cold pupil images of $40\ \mu\text{m}$ changes the plate-scale by 0.03% and thus shifts the image at the corner of the fringe tracking field by 0.014 arcsec or 2.8 pixel and thus a reduction in R23 of 5% in the K band.

Similarly, a difference in the separation of the two cold pupil images will result in a static piston $\text{OPD}(\alpha)$ between the two pupils as a function of the position α in the field of view. For an error in the separation of the two cold pupils of Δs , the introduced static piston is $\text{OPD}(\alpha) = \Delta s \times \tan(\alpha \cdot 66.66)$. As an example, for $\Delta s = 40\ \mu\text{m}$, the static piston between the edges of the fringe tracking field and the science detector is $0.6\ \mu\text{m}$. Using figure 7, this can be converted into a reduction of R23 of 1%.

4. CONCLUSION

In this paper we showed that the Strehl-ratio or fringe contrast is not sufficient for a concise performance evaluation of a Fizeau interferometer, like LINC-NIRVANA. For this reason a new metric to define the performance of such an instrument was presented. This method is based on analyzing the power contained in the high angular frequencies, which are accessible only with the interferometer, but not with the individual telescopes. We defined the ratio R23 between the power contained in these angular frequencies in the actual image and that of a perfect telescope and instrument without atmospheric disturbances as a new metric for evaluating the performance of the instrument. We furthermore presented some applications for various effects on the performance of LINC-NIRVANA, like the influence of wavefront aberrations, field rotation, piston variations, atmospheric dispersion, offsets between the rotation and the optical axis, filter bandwidth, and showed how these results can be used to derive the specifications on the shape of the cold pupil images inside the instrument.

REFERENCES

1. T. Herbst, R. Ragazzoni, A. Eckart, and G. Weigelt, "LINC-NIRVANA: the Fizeau interferometer for the LBT," *7013*, SPIE, 2008.
2. J. Farinato, R. Ragazzoni, C. Arcidiacono, G. Gentile, A. Brunelli, V. Viotto, E. Diolaiti, I. Foppiani, M. Lombini, L. Schreiber, P. Bizenberger, F. de Bonis, S. Egner, W. Gaessler, T. Herbst, M. Kuerster, L. Mohr, and R.-R. Rohloff, "The multiple field-of-view layer-oriented wavefront sensing system of LINC-NIRVANA: two arcminutes of corrected field using solely natural guide stars," *7015*, SPIE, 2008.
3. T. Bertram, A. Eckart, B. Lindhorst, S. Rost, C. Straubmeier, Y. Wang, I. Wank, G. Witzel, U. Beckmann, M. Brix, S. Egner, and T. Herbst, "The LINC-NIRVANA fringe and flexure tracking system," in *SPIE*, *7013*, 2008.
4. K.-H. Hofmann, T. Driebe, M. Heininger, D. Schertl, and G. Weigelt, "Aperture synthesis imaging with the LBT: reconstruction of diffraction-limited images from LBT LINC-NIRVANA data using the Richardson-Lucy and regularized building block method," *6272*, SPIE, 2006.
5. B. Anconelli, M. Bertero, P. Boccacci, M. Carbillet, and H. Lanteri, "Restoration of interferometric images. III. Efficient Richardson-Lucy methods for LINC-NIRVANA data reduction," *A&A* **430**, p. 731, 2005.
6. P. Bizenberger, E. Diolaiti, S. Egner, T. Herbst, R. Ragazzoni, D. Reymann, and W. Xu, "LINC-NIRVANA: Optical design of an interferometric imaging camera," in *SPIE*, *6269*, 2006.
7. S. Ligorì, R. Lenzen, H. Mandel, B. Grimm, and U. Mall, "The MPIA detector system for the LBT instruments LUCIFER and LINC-NIRVANA," *5499*, p. 108, SPIE, 2004.
8. W. Traub, "Combining beams from separated telescopes," *Appl. Opt.* **25**, p. 528, 1986.